THE JOURNAL OF PHYSICAL CHEMISTRY B

Article

pubs.acs.org/JPCB

Isolation of a Highly Reactive β-Sheet-Rich Intermediate of Lysozyme in a Solvent-Free Liquid Phase

Alex P. S. Brogan, Kamendra P. Sharma, Adam W. Perriman,* and Stephen Mann

Centre for Organized Matter Chemistry, School of Chemistry, University of Bristol, Bristol BS8 1TS, United Kingdom

Supporting Information

ABSTRACT: The thermal denaturation of solvent-free liquid lysozyme at temperatures in excess of 200 °C was studied by synchrotron radiation circular dichroism spectroscopy. Temperature-dependent changes in the secondary structure were used to map the equilibrium denaturation pathway and characterize a reactive β-sheet-rich unfolding intermediate that was stable in the solvent-free liquid phase under anhydrous conditions but which underwent irreversible aggregation in the presence of water. The unfolding intermediate had a transition temperature of 78 °C and was extremely stable to temperature, eventually reaching the fully denatured state at 178 °C. We propose that the three-stage denaturation pathway arises from the decreased stability of the native state due to the absence of any appreciable hydrophobic effect, along with an entropically derived stabilization of the reactive intermediate associated with molecular crowding in the solvent-free liquid.

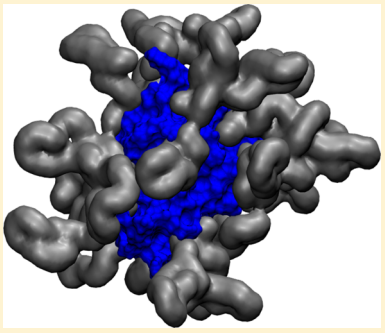

INTRODUCTION

Water molecules are of fundamental importance for the structural preservation, dynamics, folding, and function of proteins. Solvation contributes significantly to the hydrophobic effect and plays a key role in modulating the electrostatic, van der Waals, and internal hydrogen bonding interactions that collectively give rise to the high-fidelity conservation of globular architectures and protein folding pathways in water.[1−4] Moreover, critical levels of hydration, typically 0.2−0.4 g/g water/protein, are considered to be essential for functional protein dynamics, which give rise to moderate levels of enzyme activity when dry protein powders are dispersed in nonaqueous solvents.[5−12]

Given this consensus, recent studies on the synthesis and characterization of solvent-free liquid proteins[13] provide a timely opportunity to investigate the universality of hydration in the formation of stable protein structures, maintenance of function, and facilitation of unfolding and refolding pathways. These novel biomolecular fluids are prepared by ambient temperature melting of lyophilized powders comprising discrete nanoscale constructs synthesized by electrostatic conjugation of anionic polymer surfactants to the surface of cationized proteins such as ferritin[14] and myoglobin[15] or cationized plant virions.[16] Significantly, minimal loss of secondary structure is observed when aqueous solutions of the surface-engineered cationized proteins are lyophilized and melted into the solvent-free liquid state. As a consequence, the myoglobin melts retain their ability to perform reversible oxygen binding under almost anhydrous conditions (<0.1 wt % of water).[15] Moreover, the solvent-free myoglobin liquids exhibit remarkable thermal stability with a half denaturation temperature (T_m) of approximately 160 °C compared with 70 °C in aqueous solution. Remarkably, samples heated to T_m and then cooled to room temperature show 95% refolding of the myoglobin molecules in the solvent-free state, challenging the centrality of hydration in folding pathways.[17] A mechanistic explanation for these observations has been proposed on the basis of temperature-dependent elastic incoherent neutron scattering experiments.[18] These studies indicate that the polymer surfactant coronal layer has sufficient conformational freedom to act as a surrogate solvent shell, and as a consequence the dynamical fluctuations of myoglobin in the solvent-free liquid state are very similar to those observed for the aqueous protein.

Based on these recent observations, it seems feasible that solvent-free liquid proteins could provide a novel opportunity to access intermediate folding states that normally undergo irreversible aggregation in aqueous media,[19−22] but which might be stabilized in water-free protein melts. In this regard, the folding pathway of lysozyme (Lyz, M_w = 14 300) and mechanisms of irreversible aggregation of intermediate folded states into amyloid fibres have been extensively studied,[19,20,23−25] although resolution and characterization of the α-helical or β-strand enriched intermediates require the use of adverse conditions such as extremely low pH or the presence of fluoroalcohols.[26,27] Here we describe for the first time the preparation and characterization of a solvent-free liquid of lysozyme and exploit the hyper-thermophilic stability of the protein melt to determine the thermally induced changes in secondary structure up to a temperature of 210 °C. In so doing, we are able to access an equilibrium intermediate state, which is stable in the solvent-free liquid but highly reactive toward aggregation in the presence of water.

Received: April 26, 2013
Revised: June 18, 2013
Published: June 21, 2013

dx.doi.org/10.1021/jp4041524 | J. Phys. Chem. B 2013, 117, 8400−8407

EXPERIMENTAL METHODS

Preparation of Solvent-Free Liquid Lysozyme. The synthesis of solvent-free liquid [C-Lyz][S_2] was performed as described previously for solvent-free liquid myoglobin.[15] Briefly, *N*,*N*′-dimethyl-1,3-propanediamine (DMPA) was coupled to the side chains of the acidic amino acid residues of hen egg white lysozyme (Lyz, Sigma U.K.) via carbodiimide activation. After dialysis against Milli-Q water for 48 h and centrifugation, the resultant C-Lyz solution was added to a solution (pH 6.8, 10 mg mL^{-1}) containing an excess of ethylene glycol ethoxylate lauryl ether (S_2 = $CH_3(CH_2)_xO$-$(CH_2CH_2O)_nCH_2COOH$; x = 11−13, n = 10, Sigma U.K.) and stirred for 12 h to produce an aqueous solution of [C-Lyz][S_2] nanoconjugates. Unbound surfactant molecules were removed by dialysis against Milli-Q water for 48 h, and the resultant solution was lyophilized for 48 h to remove water. This yielded a low density powder which upon thermal annealing yielded a pale yellow solvent-free liquid [C-Lyz][S_2].

Circular Dichroism Spectroscopy. Temperature-dependent synchrotron radiation circular dichroism (SRCD) spectra of solvent-free liquid [C-Lyz][S_2] were collected on beamline B23 at the Diamond Light source, with a wavelength range of 165−260 nm, integration time of 2 s, and a 1 nm data interval. Samples were cast as thin films between two synthetic quartz plates, and the temperature was controlled by using a modified Linkam thermal stage. Temperature-dependent CD spectra of aqueous solutions of [C-Lyz][S_2] and C-Lyz were recorded between 260 and 190 nm on a Jasco J-810/5 spectrometer with a Jasco PTC-423 peltier stage. A path length of 1 mm path and scan rate of 50 nm min^{-1} with a minimum of 4 accumulations was used. Concentrations of the protein solutions were determined using a Perkin-Elmer Lambda 25 UV/vis spectrometer.

Secondary structure estimation was performed using the DICHROWEB[28] service with the CDSSTR algorithm[29] and associated basis sets.[30,31] Spectra were fitted between 190 and 240 nm, with resultant fits only accepted when the normalized root mean squared deviations were below 0.05. For the solvent-free liquids, the path length was estimated by casting a known mass of sample over a known area.

Thermal Denaturation Studies. Equilibrium thermal denaturation experiments on solvent-free liquid [C-Lyz][S_2] were measured using SRCD spectroscopy from 25 to 210 °C with full spectra recorded every 5 °C after 5 min equilibration. Equivalent studies on aqueous solutions of Lyz, C-Lyz, and [C-Lyz][S_2] were conducted over a temperature range of 25 to 95 °C at a ramp rate of 0.5 deg min^{-1}, with the intensity at 222 nm recorded every 1 °C and full spectra every 5 °C. Thermodynamic parameters were determined according to established procedures for 2- and 3-state models of thermal denaturation.

Thermal Denaturation Thermodynamics. Thermodynamic parameters for the aqueous systems were evaluated by applying a two-state model to the thermal denaturation data,[32−35] which describes the equilibrium between the native state (N) and the denatured state (D) where the population of each state is defined by the equilibrium constant (K_D)

$$\mathrm{N} \overset{K_D}{\rightleftharpoons} \mathrm{D} \tag{1}$$

To calculate the position on the equilibrium thermal denaturation pathway, the intensity of the negative circular dichroic peak at 222 nm was used as an order parameter (y) to express the fraction denatured (f_D)

$$f_D = \frac{(y - y_N)}{(y_D - y_N)} \tag{2}$$

where y_N and y_D are the intensites of the 222 nm peak in the native state and denatured state, respectively. The equilibrium constant of denaturation is therefore given by

$$K_D = \frac{f_D}{1 - f_D} \tag{3}$$

and the Gibbs free energy of denaturation (ΔG_D) calculated from

$$\Delta G_D = -RT \ln K_D \tag{4}$$

ΔG_D was plotted as a function of temperature and the transition region fitted using linear regression; the half-denaturation temperature (T_m) was evaluated using the x-axis intercept (ΔG_D = 0), and the entropy (ΔS_m) and enthalpy (ΔH_m) at the half-denaturation temperature were evaluated from the gradient of the linear transition region, and the product of the half-denaturation temperature (T_m) and entropy (ΔS_m), respectively, according to

$$\Delta G_m = 0 = \Delta H_m - T_m \Delta S_m \tag{5}$$

under these conditions.

Thermodynamic parameters for solvent-free liquid [C-Lyz][S_2] were calculated using a 3-state model based on two distinct transitions,[27] i.e., N→I and I→D (where I is the intermediate state). Using eqs 2 and 3, this provided K_{NI} and K_{ID}, which allowed for the extraction of f_N, f_I, and f_D with the following relationships:

$$f_N = \frac{1}{1 + K_{NI} + K_{NI}K_{ID}}$$

$$f_I = \frac{K_{NI}}{(1 + K_{NI} + K_{NI}K_{ID})}$$

$$f_D = 1 - f_N - f_I$$

ΔG_{NI} and ΔG_{ID} were calculated with eq 4 and plotted as functions of temperature, with the transition region fitted using linear regression, to determine the respective transition temperatures, enthalpies, and entropies.

Scattering Techniques. Small angle neutron scattering (SANS) on the solvent-free liquid samples was conducted on the LoQ beamline at ISIS, with samples cast in 2-part quartz cells with path lengths of 1 mm. SANS experiments on the aqueous samples were conducted on the D22 beamline at ILL, with samples prepared in D_2O and measured in 1 mm path length glass cuvettes. Data was fitted using Igor Pro 6.31, with the NIST NCNR SANS macro package.[36] Wide angle X-ray scattering (WAXS) was conducted in the School of Physics, University of Bristol. Solvent-free liquid samples were cast as films between two brass washers with mica windows, and aqueous solutions were placed in quartz capillaries. Dynamic light scattering (DLS) profiles were measured in a Malvern Instruments Zetasizer ZS, with samples in glass cuvettes (1 cm path length) and protein concentrations of 1 mg mL^{-1}.

Characterization. Polarized light microscopy was performed in transmission mode on a Leica Inverted Microscope

dx.doi.org/10.1021/jp4041524 | J. Phys. Chem. B 2013, 117, 8400−8407

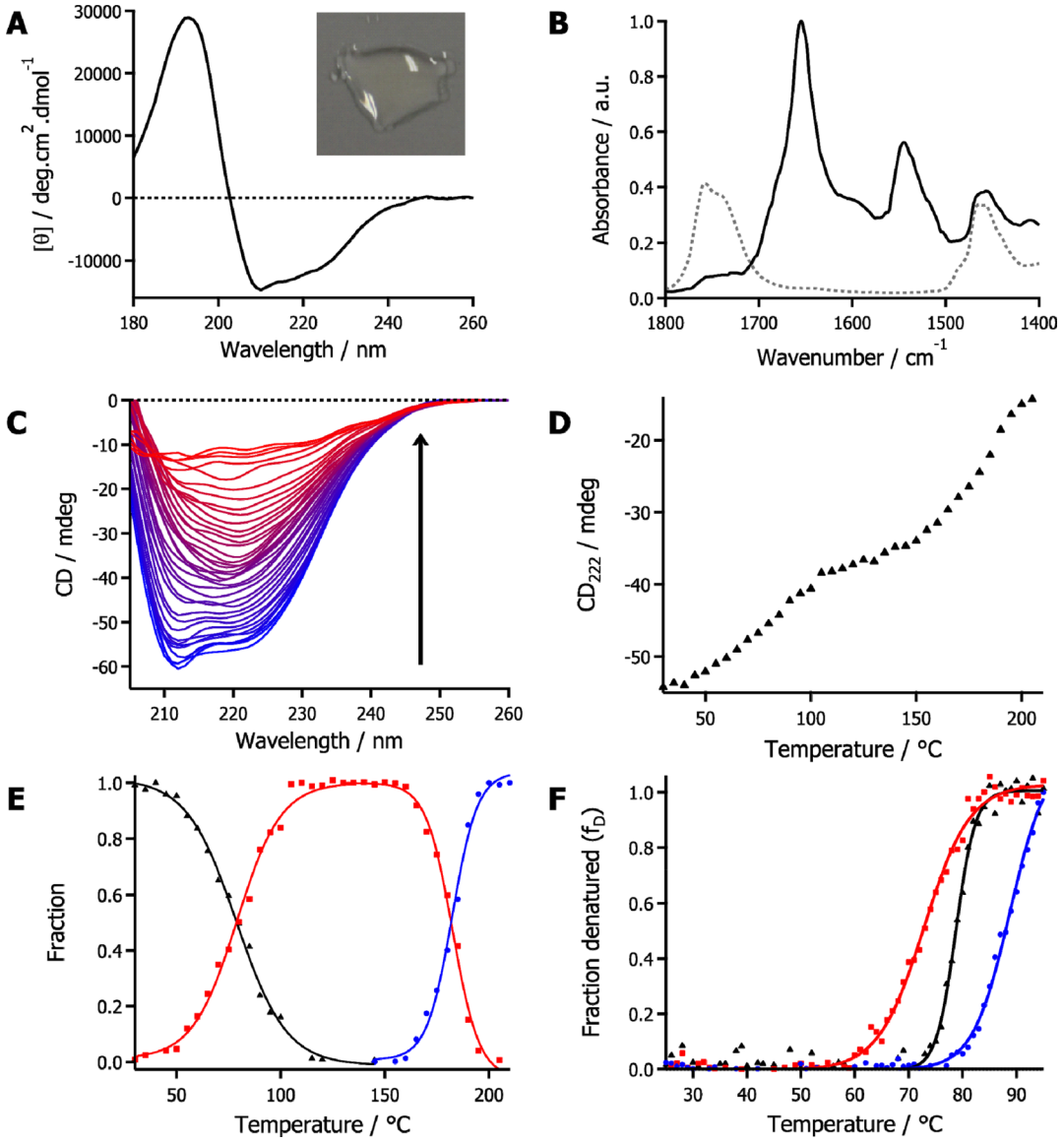

Figure 1. (A) SRCD spectrum showing far-UV region for solvent-free liquid [C-Lyz][S_2] measured at 30 °C. Inset shows optical image of the solvent-free liquid at 30 °C. (B) ATR-FTIR spectra showing amide region for solvent-free liquid [C-Lyz][S_2] (black) and adsorption bands for anhydrous S_2 (gray dashed). (C) SRCD spectra of solvent-free liquid [C-Lyz][S_2] showing reduction in the intensity of the bands at 208 and 222 nm over a temperature range of 25 (blue) to 210 °C (red) at 10 °C intervals. Arrow indicates increase in temperature. (D) Plot of CD peak intensity at 222 nm for solvent-free liquid [C-Lyz][S_2] at temperatures between 25 and 210 °C showing the presence of an intermediate state in the unfolding pathway. (E) Temperature-dependent plots showing fractions of native (f_N, black triangles; sigmoid fit, black line), intermediate (f_I, red squares; sigmoid fit, red line), and denatured (f_D, blue circles; sigmoid fit, blue line) states for solvent-free liquid [C-Lyz][S_2]; values were determined by deconvolution of plot shown in (D). (F) Temperature-dependent plots showing fraction of denatured state (f_D) for aqueous solutions of Lyz (black triangles, sigmoid fit black line), [C-Lyz] (red squares, sigmoid fit red line), and [C-Lyz][S_2] (blue circles, sigmoid fit blue line); values were determined from SI Figure S5.

DMI3000 B with samples cast onto glass slides. Cryo-TEM was performed on a JEOL TEM 2010 with a L-N_2 cooling stages. Samples were prepared on carbon coated copper grids, stained with uranyl acetate, and frozen with liquid nitrohgen.

Differential scanning calorimetry (DSC) of solvent-free liquid [C-Lyz][S_2] was run between −70 and +70 °C at a heating/cooling rate of 10 °C min^{-1} on a TA Instruments Q100 DSC. Thermogravimetic analysis (TGA) of solvent-free liquid [C-Lyz][S_2] was performed from 25 to 800 °C at 10 °C min^{-1} on a TA Instruments Q500 thermogravimetric analyzer. The temperature was held at 80 °C for 1 h to eliminate atmospheric water from the sample and then held at 110 °C for 1 h to assess the water content.

Fluorescence excitation and emission spectra were collected using a Jasco FP-6500 spectrofluorometer. Samples were run in quartz fluorescence cuvettes.

RESULTS AND DISCUSSION

Electrostatic grafting of the polymer surfactant $CH_3(CH_2)_xO$-$(CH_2CH_2O)_nCH_2COOH$ (S_2 ; x = 11−13, n = 10) to cationized lysozyme (C-Lyz) in aqueous solution gave a discrete, water-soluble nanoconstruct ([C-Lyz][S_2]). Extensive lyophilization of a dialyzed aqueous solution of [C-Lyz][S_2] yielded a waxy solid which melted at 22 °C (SI, Figure S1) to form a pale-yellow viscous solvent-free liquid (Figure 1A,

dx.doi.org/10.1021/jp4041524 | J. Phys. Chem. B 2013, 117, 8400−8407

Table 1. Thermodynamic Values for the Denaturation of Aqueous [C-Lyz][S_2] and Solvent-Free [C-Lyz][S_2] Conjugates at Their Respective Denaturation Temperatures (T_m)[a]

	T_m/°C	ΔS_m/J K^{-1} mol^{-1}	ΔH_m/kJ mol^{-1}	ΔG(87.8 °C)/kJ mol^{-1}	$T\Delta S$(87.8 °C)/kJ mol^{-1}	ΔH(87.8 °C)/kJ mol^{-1}
aqueous	87.8	974 ± 39	351 ± 25	0	351 ± 25	351 ± 25
solvent-free N → I	78.2	245 ± 9.7	86 ± 5.9	−2.4 ± 0.1	88.5 ± 0.01	86.2 ± 0.1
solvent-free I → D	178.2	310 ± 19.4	140 ± 12.4			
solvent-free N → D		555 ± 21.7	226 ± 13.7			

[a]All parameters were calculated from plots of free energy as calculated from measurements of the intensity of the 222 nm band using CD spectroscopy (SI Figure 7). For the solvent-free N → D transition, this was calculated as the sum of the individual contributions.

inset). Thermogravimetric analysis gave a water content of 0.14 wt % (SI, Figure S2), corresponding to 3 water molecules per protein−polymer surfactant construct, 2 orders of magnitude lower than the ∼900 water molecules required to form a monolayer on the surface of the protein.[37] UV/vis spectroscopy of the redissolved [C-Lyz][S_2] melt indicated that 26 S_2 chains were electrostatically attached to the protein surface to produce a discrete and stoichiometric construct (SI, Figure S3). SRCD spectroscopy of the solvent-free liquid [C-Lyz][S_2] showed negative bands at 222 and 208 nm and a positive feature at 195 nm, indicative of a predominately α-helical protein (Figure 1A). Deconvolution of the spectrum gave α-helix and β-sheet estimated contents of 40% and 20%, respectively. These values were essentially unchanged from the more quantitatively robust values determined for aqueous solutions of [C-Lyz][S_2] (38% and 13%), C-Lyz (35% and 15%), and native Lyz (35% and 15%) (SI, Figure S4), indicating that the protein secondary structure was retained in the liquid state in the absence of water. This was confirmed by ATR-FTIR spectroscopy, which showed strong amide I and II bands at 1655 and 1545 cm^{-1} respectively, typical for predominately α-helical proteins (Figure 1B).

Based on previous results that showed hyper-thermophilic behavior in solvent-free liquids of myoglobin,[17] we used SRCD spectroscopy to investigate the thermal stability of the solvent-free [C-Lyz][S_2] melts and to determine the pathway of protein unfolding over an extensive temperature range not restricted by solvent boiling or the requirement for auxiliary chemical denaturants. Thermal denaturation of solvent-free liquid [C-Lyz][S_2] was monitored by measuring the reduction in peak intensity at 208 and 222 nm as the temperature was increased from 25 °C. The data indicated that complete denaturation of the [C-Lyz][S_2] construct was only achieved when the temperature reached 210 °C (Figure 1C), indicating high thermal stability with regard to protein unfolding in the solvent-free liquid state. In contrast, native Lyz, C-Lyz, and [C-Lyz][S_2] were fully denatured in aqueous solutions at temperatures below 95 °C (SI, Figure S5). Interestingly, temperature-dependent plots of the intensity at 222 nm indicated that there was an observable equilibrium intermediate on the thermal denaturation pathway of the solvent-free [C-Lyz][S_2] conjugate (Figure 1D). These plots were used to determine the fraction of native (N), intermediate (I), and denatured (D) states across the temperature range, which indicated that the N → I and I → D transition temperatures in the solvent-free state were 78 and 178 °C, respectively (Figure 1E). In contrast, a three-state unfolding pathway was not observed for solvent-free myoglobin,[17] or for Lyz, [C-Lyz], or [C-Lyz][S_2] in aqueous solution; the latter displayed classical two-state thermal denaturation curves with half denaturation temperatures (T_m) of 79, 72, and 88 °C respectively (Figure 1F).

Plots of free energy of denaturation against temperature were determined for the two-state transitions for aqueous Lyz, C-Lyz and [C-Lyz][S_2], as well as for the N → I and I → D transitions associated with protein unfolding in the solvent-free [C-Lyz][S_2] construct (SI, Figure S6). Comparing the thermodynamic parameters for aqueous or solvent-free liquid states of [C-Lyz][S_2], the native state of the latter was less stable with respect to the solvent-free intermediate state than the native aqueous state was to the aqueous denatured state by 2.4 kJ mol^{-1} (Table 1). The destabilization could be due to the increased hydrophobicity of the solvent-free state, which would decrease the energy barrier associated with exposure of unfolded apolar amino acid residues through favorable interactions with the polymer surfactant shell. This was consistent with a marked reduction of the positive enthalpy of denaturation of solvent-free [C-Lyz][S_2] ($\Delta H_{N\rightarrow I}$ = 86 J K^{-1} mol^{-1}) as compared to the aqueous nanoconjugate (ΔH_m = 351 J K^{-1} mol^{-1}; Table 1). However, the enthalpic differences were in part offset by the considerably lower change in entropy associated with partial unfolding in the molecularly crowded environment of the viscous solvent-free fluid ($\Delta S_{N\rightarrow I}$ = 245 J K^{-1} mol^{-1}, ΔS_m = 974 J K^{-1} mol^{-1}, Table 1). Indeed, this entropic constriction appeared to be the primary reason for stabilization of the intermediate state over an extended temperature range as the change in entropy associated with denaturation of the intermediate was also relatively low in value ($\Delta S_{I\rightarrow D}$ = 310 J K^{-1} mol^{-1}, Table 1).

The above results indicated that the presence of the equilibrium intermediate occurred by a destabilization of the native state of [C-Lyz][S_2] through reduction of the enthalpic barrier to denaturation, which was concurrent with entropic stabilization of the partially unfolded state. The presence of equilibrium intermediates during Lyz denaturation has also been demonstrated under conditions of extremely low pH[27] or in the presence of 2,2,2-trifluoroethanol.[26] In general, observable intermediates in Lyz denaturation have been shown to be enriched in α-helical[26,38] or β-sheet domains,[20] depending on whether they represent the rate limiting step of lysozyme folding or a pathway to amyloid fibril formation, respectively. In this regard, we used temperature-dependent SRCD and ATR-FTIR spectroscopies to investigate the structure of the [C-Lyz][S_2] intermediate as well as the reversibility of the associated unfolding/folding pathway in the solvent-free liquid. CD spectra recorded above the N → I transition temperature showed a distinct loss of the α-helical content (bands at 222 and 208 nm), and concomitant formation of a single band at 216 nm corresponding to a considerable increase in the β-sheet secondary structure content associated with the intermediate state (Figure 2A). Significantly, CD spectra of the liquid protein heated to 110 °C for 10 min and then cooled to 30 °C showed no evidence for recovery of the N state (Figure 2A), while thermal treatment of

dx.doi.org/10.1021/jp4041524 | J. Phys. Chem. B 2013, 117, 8400−8407

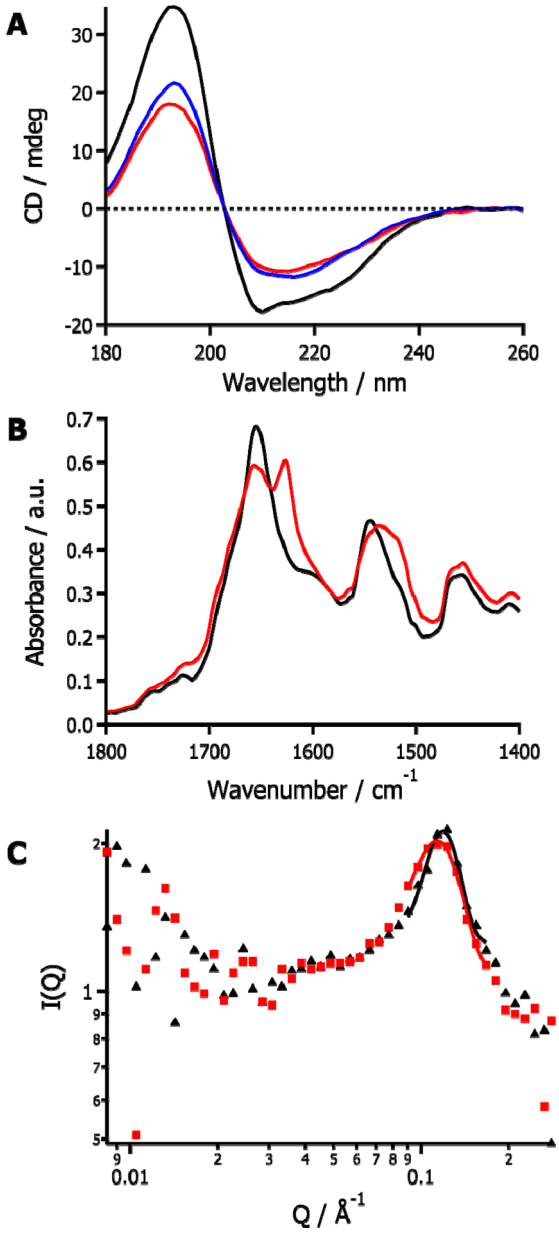

Figure 2. (A) SRCD spectra showing solvent-free liquid [C-Lyz][S_2] at 30 (black), 110 (red), and after heating to 110 °C followed by cooling to 30 °C (blue) showing absence of renaturation in the cooled sample. (B) ATR-FTIR spectra showing solvent-free liquid [C-Lyz][S_2] at room temperature (black) and after incubation at 120 °C and cooling to room temperature (red) showing irreversibility of the intermediate formed at 120 °C. (C) SANS profile of solvent-free liquid [C-Lyz][S_2] at 30 °C (black) and after incubation at 120 °C and cooling to 30 °C (red) showing protein−protein correlation distances fitted with Gaussian curves.

samples below 78 °C showed reversible refolding (SI, Figure S7). This was consistent with corresponding ATR-FTIR spectra of the solvent-free liquid [C-Lyz][S_2] intermediate recorded at room temperature and after heating to 120 °C for 60 min followed by recooling to room temperature (Figure 2B). The data showed that thermal processing resulted in the presence of a new amide I peak at 1627 cm^{-1} along with broadening and shifting of the amide II peak to a value of 1533 cm^{-1}, indicative of the irreversible formation of a predominantly antiparallel β-sheet intermediate above 78 °C. Similar studies undertaken on solvent-free samples held at 120 °C for 6 h prior to cooling to room temperature showed no further change in the secondary structure confirming that the intermediate was thermodynamically stable under these conditions (SI, Figure S8).

Small angle neutron scattering (SANS) was undertaken to investigate global changes in structure associated with formation of the intermediate protein conformation in solvent-free liquids of [C-Lyz][S_2] heated to 120 °C for 60 min and subsequently cooling to 30 °C (Figure 2C). Profiles of the as-prepared fluid gave a protein−protein correlation peak at 0.119 $Å^{-1}$ corresponding to a center-to-center distance between neighboring protein−polymer surfactant constructs of 52.7 (±0.4) Å, which was consistent with the radius of the aqueous conjugates (29 Å) determined by using a core−shell model to fit the corresponding SANS data (SI, Figure S9), albeit with potential interdigitation between adjacent coronas. Upon formation of the intermediate, this interparticle separation changed slightly with the correlation peak shifting to 0.114 $Å^{-1}$, corresponding to an increase in distance to 55.3 (±0.3) Å. Although this represented a slight increase in the radius of lysozyme core due to partial denaturation, this implied an increase in volume occupied by the protein−polymer surfactant constructs in the intermediate state, that was compatible with considerable rearrangement of the coronal layer and presence of longer range interactions between neighboring constructs. Both these factors would facilitate irreversibility in the N → I transition above 78 °C.

Demonstration of irreversibility in the solvent-free liquid state was in stark contrast to investigations previously undertaken on solvent-free liquids of myoglobin, which showed refolding behavior when the thermally denatured protein−polymer surfactant constructs were cooled from the half denaturation temperature to 30 °C.[17] Likewise, denaturation of aqueous [C-Lyz][S_2] was followed by complete renaturation when thermally cycled between 25 and 95 °C (SI, Figure S10). We attribute these differences to the increased entropic stabilization of the intermediate state in the solvent-free state (see above discussion), and the increased β-sheet content of the partially denatured [C-Lyz][S_2] conjugate. Together, these factors were consistent with a denaturation pathway described by the Lumry-Eyring model[39,40] in which a native (N) state is in equilibrium with an initial equilibrium intermediate (I_i) that undergoes a thermally activated irreversible transformation to a final intermediate state (I_f) prior to formation of the fully denatured state (N = [I_i → I_f] → D).

Interestingly, the high level of stability of the final intermediate produced in the heated solvent-free [C-Lyz][S_2] conjugate not only prevented access to the native state but also curtailed transformation of the β-sheet enriched intermediate into higher-order aggregates that are typically observed under aqueous conditions. This was evidenced by a minimal change in the optical properties of the solvent-free liquid [C-Lyz][S_2] after formation of the intermediate phase at 120 °C (SI, Figure S11), DSC profiles for the intermediate that showed similar melting temperatures when compared with the as-prepared materials (SI, Figure S12), and SANS data that indicated no change in the protein−protein correlation distance and no evidence of increased scattering at low Q (Figure 2C). In addition, wide-angle X-ray scattering (WAXS) profiles showed a single scattering peak centered at 1.48 $Å^{-1}$ for both the native and intermediate forms of the solvent-free [C-Lyz][S_2] conjugate (SI, Figure S13). The peak corresponded to a d spacing of 4.26 Å that was attributed to the polymer surfactant

dx.doi.org/10.1021/jp4041524 | J. Phys. Chem. B 2013, 117, 8400−8407

alkyl−alkyl separations as confirmed by scattering profiles of S_2 alone (SI, Figure S13). No peaks were observed for intermolecular β-sheet formation (4.7 Å [1.33 $Å^{-1}$]), indicating that higher-order amyloid-like aggregates were not produced in the thermally treated solvent-free liquids.

While the as-prepared solvent-free liquid protein readily dissolved in water at room temperature to produce transparent solutions, addition of water to melts thermally processed at 120 °C produced opaque dispersions. DLS studies showed an increase in mean hydrodynamic radius of the redissolved [C-Lyz][S_2] from 2.4 to 19 nm after incubation at 120 °C (Figure 3A), indicating that aggregation of the partially denatured protein intermediate was strongly promoted in the presence of water. Corresponding images recorded by cryo-TEM showed beam-sensitive amorphous aggregates with sizes ranging from 10 to 90 nm with a mean size of 30 (±9) nm (Figure 3B). CD spectroscopy confirmed that the predominantly β-sheet secondary structure of the intermediate was retained in the water-dispersed aggregates (Figure 3C), although staining with the fluorescent probe ThT did not indicate any evidence for an amyloid-like nanostructure (SI, Figure S14). This was consistent with WAXS data that showed no intermolecular β-sheet feature at 1.33 $Å^{-1}$ (4.7 Å) for the redissolved thermally treated samples (SI, Figure S15). Instead, the profile showed an apparent scattering maximum at 1.98 $Å^{-1}$ (3.17 Å) corresponding to a polarity-induced contraction in the surfactant alkyl−alkyl separation in the aqueous phase compared with the solvent-free liquid state (4.26 Å). This peak was also present in the WAXS profile of the redissolved as-prepared sample, although the scattering intensity was considerably decreased due to the nonaggregated state of the solution.

CONCLUSIONS

In this paper, we use conjugation chemistry to molecularly engineer the surface of Lyz such that exhaustive extraction of water produces anhydrous powders that can be thermally melted into a solvent-free liquid state. The latter consists of structurally intact cationized Lyz molecules comprising an electrostatically coupled coronal layer of 26 polymer−surfactant anions that facilitate melting in the absence of protein degradation. Moreover, the hybrid [C-Lyz][S_2] conjugates exhibit hyper-thermophilic behavior in the solvent-free state but not when re- dispersed in aqueous solution. Significantly, we demonstrate that the high thermal stability of the solvent-free [C-Lyz][S_2] constructs can be exploited to trap an intermediate state on the unfolding pathway that is stable with respect to higher-order assembly in the solvent-free liquid but highly reactive toward aggregation in the presence of water. The initial intermediate is in equilibrium with the native state below 78 °C but transforms into an irreversible β-sheet-enriched state at higher temperature that does not refold on cooling and transforms into the fully denatured construct [C-Lyz][S_2] at a half denaturation temperature of 178 °C. We attribute the three-stage pathway to the decreased stability of the native state in the absence of any appreciable hydrophobic effect, along with an entropically derived stabilization of the intermediate due to molecular constriction in the solvent-free liquid. As a consequence, stabilization of the β-sheet intermediate state within a grafted polymer surfactant anhydrous corona suggests that solvent-free liquid proteins could be useful in general to isolate new structural intermediates of protein unfolding and lead to a greater understanding of transient analogues in aqueous conditions. In so doing, this may offer a procedure for decoupling solvent effects from the multiple forces responsible for the irreversible assembly of proteins into higher-order structures, and provide greater understanding of the molecular pathways to protein aggregation in the isolation of relevant intermediates.

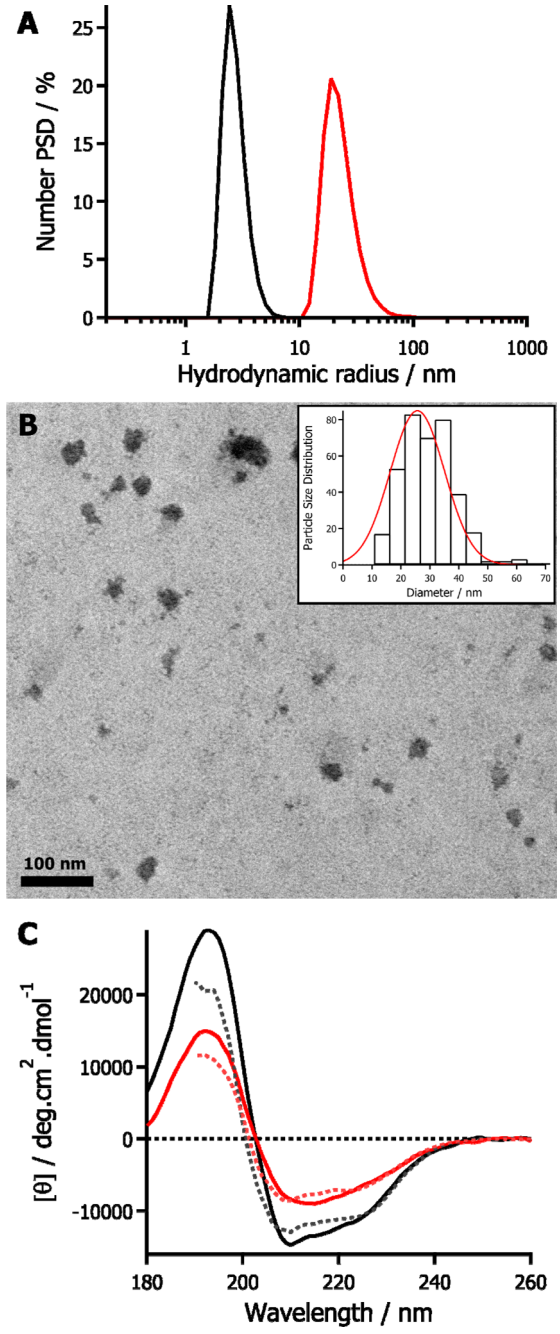

Figure 3. (A) DLS-derived number particle size distributions for redissolved as-prepared [C-Lyz][S_2] (1 mg mL^{-1}, 40 mM phosphate buffer pH 6.8) (black), and after incubation at 120 °C, cooling to room temperature and dissolution in water (red). (B) Uranyl acetate stained cryo-TEM image showing aggregates of [C-Lyz][S_2] after incubation at 120 °C, and dissolving in water at room temperature (10 mg mL^{-1}); inset showing corresponding particle size distribution of [C-Lyz][S_2] aggregates. (C) CD spectra showing mean residue ellipticity of solvent-free liquid [C-Lyz][S_2] at 30 °C (solid black) and after thermal treatment at 120 °C and cooling to room temperature (solid red). Corresponding spectra after redissolution of these samples in water at 30 °C are also shown (black/red dashed lines).

dx.doi.org/10.1021/jp4041524 | J. Phys. Chem. B 2013, 117, 8400−8407

■ ASSOCIATED CONTENT

Supporting Information

Thermal analysis of the solvent-free liquid protein, stoichiometry determination, CD spectra of aqueous samples, thermal denaturation and refolding of aqueous samples, refolding of solvent-free liquid, plots of free energy against temperature, optical microscopy, SANS of aqueous samples, WAXS, and fluorescence. This material is available free of charge via the Internet at http://pubs.acs.org.

■ AUTHOR INFORMATION

Corresponding Author

*E-mail: chawp@bristol.ac.uk.

Notes

The authors declare no competing financial interest.

■ ACKNOWLEDGMENTS

We thank the EPSRC (Cross-disciplinary Interfaces Program) and ERC (Advanced Grant) for financial support, the Diamond Light Source for access to the B23 beamline (SRCD), ISIS for use of the LOQ beamline (SANS), and ILL for access to the D22 beamline (SANS). We thank Dr. Paul Brown and Mr. Greg Smith for help with SANS, Prof. Rob Richardson for assistance with WAXS, and Mr. Jon Jones for help with cryo-TEM.

■ REFERENCES

(1) Dill, K. A. Dominant Forces in Protein Folding. *Biochemistry* **1990**, *29*, 7133−7155.
(2) Szilágyi, A.; Závodszky, P. Structural Differences Between Mesophilic, Moderately Thermophilic and Extremely Thermophilic Protein Subunits: Results of a Comprehensive Survey. *Structure* **2000**, *8*, 493−504.
(3) Das, R.; Gerstein, M. The Stability of Thermophilic Proteins: a Study Based on Comprehensive Genome Comparison. *Funct. Integr. Genomics* **2000**, *1*, 76−88.
(4) Xiao, L.; Honig, B. Electrostatic Contributions to the Stability of Hyperthermophilic Proteins. *J. Mol. Biol.* **1999**, *289*, 1435−44.
(5) Dominguez De Maria, P. Nonsolvent Applications of Ionic Liquids in Biotransformations and Organocatalysis. *Angew. Chem., Int. Ed.* **2008**, *47*, 6960.
(6) van Rantwijk, F.; Sheldon, R. A. Biocatalysis in Ionic Liquids. *Chem. Rev.* **2007**, *107*, 2757−85.
(7) Pace, C. N.; Treviño, S.; Prabhakaran, E.; Scholtz, J. M. Protein Structure, Stability and Solubility in Water and Other Solvents. *Philos. Trans. R. Soc., B* **2004**, *359*, 1225−34.
(8) Clark, D. S. Characteristics of Nearly Dry Enzymes in Organic Solvents: Implications for Biocatalysis in the Absence of Water. *Philos. Trans. R. Soc., B* **2004**, *359*, 1299−307.
(9) Klibanov, A. M. Improving Enzymes by Using Them in Organic Solvents. *Nature* **2001**, *409*, 241−246.
(10) Mattos, C.; Ringe, D. Proteins in Organic Solvents. *Curr. Opin. Struct. Biol.* **2001**, *11*, 761−4.
(11) Rialdi, G.; Battistel, E. Thermodynamics of Proteins in Unusual Environments. *Biophys. Chem.* **2007**, *126*, 65−79.
(12) Brovchenko, I.; Oleinikova, A. Which Properties of a Spanning Network of Hydration Water Enable Biological Functions? *ChemPhysChem* **2008**, *9*, 2695−702.
(13) Perriman, A. W.; Mann, S. Liquid Proteins-A New Frontier for Biomolecule-Based Nanoscience. *ACS Nano* **2011**, *5*, 6085−6091.
(14) Perriman, A. W.; Coelfen, H.; Hughes, R. W.; Barrie, C. L.; Mann, S. Solvent-free Protein Liquids and Liquid Crystals. *Angew. Chem., Int. Ed.* **2009**, *48*, 6242−6.
(15) Perriman, A. W.; Brogan, A. P. S.; Cölfen, H.; Tsoureas, N.; Owen, G. R.; Mann, S. Reversible Dioxygen Binding in Solvent-free Liquid Myoglobin. *Nat. Chem.* **2010**, *2*, 622−626.
(16) Patil, A. J.; McGrath, N.; Barclay, J. E.; Evans, D. J.; Cölfen, H.; Manners, I.; Perriman, A. W.; Mann, S. Liquid Viruses by Nanoscale Engineering of Capsid Surfaces. *Adv. Mater.* **2012**, *24*, 4557−63.
(17) Brogan, A. P. S.; Siligardi, G.; Hussain, R.; Perriman, A. W.; Mann, S. Hyper-thermal Stability and Unprecedented Re-folding of Solvent-free Liquid Myoglobin. *Chem. Sci.* **2012**, *3*, 1839−1846.
(18) Gallat, F.-X.; Brogan, A. P. S.; Fichou, Y.; McGrath, N.; Moulin, M.; Härtlein, M.; Combet, J.; Wuttke, J.; Mann, S.; Zaccai, G. A Polymer Surfactant Corona Dynamically Replaces Water in Solvent-Free Protein Liquids and Ensures Macromolecular Flexibility and Activity. *J. Am. Chem. Soc.* **2012**, *132*, 13168−13171.
(19) Frare, E.; Mossuto, M. F.; Laureto, P. P. de; Tolin, S.; Menzer, L.; Dumoulin, M.; Dobson, C. M.; Fontana, A. Characterization of Oligomeric Species on the Aggregation Pathway of Human Lysozyme. *J. Mol. Biol.* **2009**, *387*, 17−27.
(20) Gu, Z.; Zhu, X.; Ni, S.; Su, Z.; Zhou, H.-M. Conformational Changes of Lysozyme Refolding Intermediates and Implications for Aggregation and Renaturation. *Int. J. Biochem. Cell Biol.* **2004**, *36*, 795−805.
(21) Chiti, F.; Dobson, C. M. Amyloid Formation by Globular Proteins Under Native Conditions. *Nat. Chem. Biol.* **2009**, *5*, 15−22.
(22) Buell, A. K.; Dhulesia, A.; Mossuto, M. F.; Cremades, N.; Kumita, J. R.; Dumoulin, M.; Welland, M. E.; Knowles, T. P. J.; Salvatella, X.; Dobson, C. M. Population of Nonnative States of Lysozyme Variants Drives Amyloid Fibril Formation. *J. Am. Chem. Soc.* **2011**, *133*, 7737−43.
(23) Williams, M. A.; Thornton, J. M.; Goodfellow, J. M. Modelling Protein Unfolding: Hen Egg-white Lysozyme. *Protein Eng.* **1997**, *10*, 895−903.
(24) Ahmad, F.; Contaxis, C. C.; Bigelow, C. C. Free Energy Changes in Lysozyme Denaturation. *J. Biol. Chem.* **1983**, *258*, 7960−3.
(25) Yonezawa, Y.; Tanaka, S.; Kubota, T.; Wakabayashi, K.; Yutani, K.; Fujiwara, S. An Insight into the Pathway of the Amyloid Fibril Formation of Hen Egg White Lysozyme Obtained from a Small-angle X-ray and Neutron Scattering Study. *J. Mol. Biol.* **2002**, *323*, 237−251.
(26) D'Amico, M.; Raccosta, S.; Cannas, M.; Martorana, V.; Manno, M. Existence of Metastable Intermediate Lysozyme Conformation Highlights the Role of Alcohols in Altering Protein Stability. *J. Phys. Chem. B* **2011**, *115*, 4078−87.
(27) Sasahara, K.; Demura, M.; Nitta, K. Partially Unfolded Equilibrium State of Hen Lysozyme Studied by Circular Dichroism Spectroscopy. *Biochemistry* **2000**, *39*, 6475−82.
(28) Whitmore, L.; Wallace, B. A. DICHROWEB, an Online Server for Protein Secondary Structure Analyses from Circular Dichroism Spectroscopic Data. *Nucleic Acids Res.* **2004**, *32*, W668−73.
(29) Sreerama, N.; Woody, R. W. Estimation of Protein Secondary Structure from Circular Dichroism Spectra: Comparison of CONTIN, SELCON, and CDSSTR Methods with an Expanded Reference Set. *Anal. Biochem.* **2000**, *287*, 252−60.
(30) Lees, J. G.; Miles, A. J.; Wien, F.; Wallace, B. A. A Reference Database for Circular Dichroism Spectroscopy Covering Fold and Secondary Structure Space. *Bioinformatics* **2006**, *22*, 1955−62.
(31) Whitmore, L.; Wallace, B. A. Protein Secondary Structure Analyses from Circular Dichroism Spectroscopy: Methods and Reference Databases. *Biopolymers* **2008**, *89*, 392−400.
(32) Pace, C. N. The Stability of Globular Proteins. *Crit. Rev. Biochem.* **1975**, *3*, 1−43.
(33) Ahmad, F. On the Estimation of Stability Parameters from Heat-Induced Conformational Transition Curves of Proteins. *J. Iran. Chem. Soc.* **2004**, *1*, 99−105.
(34) Taneja, S.; Ahmad, F. Increased Thermal Stability of Proteins in the Presence of Amino Acids. *Biochem. J.* **1994**, *303*, 147−53.
(35) Sinha, A.; Yadav, S.; Ahmad, R.; Ahmad, F. A Possible Origin of Differences Between Calorimetric and Equilibrium Estimates of Stability Parameters of Proteins. *Biochem. J.* **2000**, *345*, 711−717.
(36) Kline, S. R. Reduction and Analysis of SANS and USANS Data Using IGOR Pro. *J. Appl. Crystallogr.* **2006**, *39*, 895−900.

(37) Stanley, C.; Krueger, S.; Parsegian, V. A.; Rau, D. C. Protein Structure and Hydration Probed by SANS and Osmotic Stress. *Biophy. J.* **2008**, *94*, 2777−89.
(38) Hamill, A. C.; Wang, S.-C.; Lee, C. T. Probing Lysozyme Conformation with Light Reveals a New Folding Intermediate. *Biochemistry* **2005**, *44*, 15139−15149.
(39) Sanchez-Ruiz, J. M. Protein Kinetic Stability. *Biophys. Chem.* **2010**, *148*, 1−15.
(40) Fu, L.; Villette, S.; Petoud, S.; Fernandez-Alonso, F.; Saboungi, M.-L. H/D Isotope Effects in Protein Thermal Denaturation: The Case of Bovine Serum Albumin. *J. Phys. Chem. B* **2011**, *115*, 1881−8.